# IX. PLASMA MAGNETOHYDRODYNAMICS AND ENERGY CONVERSION*


Prof. E. N. Carabateas
Prof. M. A. Hoffman
Prof. W. D. Jackson
Prof. J. L. Kerrebrock
Prof. J. R. Melcher
Prof. G. C. Oates
Prof. J. M. Reynolds III
Prof. A. H. Shapiro
Prof. J. L. Smith, Jr.
Prof. H. H. Woodson
W. H. Childs
R. S. Cooper
R. Dethlefsen
M. G. A. Drouet
D. A. East
F. W. Fraim III
N. Gothard
W. H. Heiser
F. D. Ketterer
G. B. Kliman
P. Klimowski
A. G. F. Kniazzeh
M. F. Koskinen
A. T. Lewis
H. D. Meyer
W. T. Norris
C. R. Phipps, Jr.
E. S. Pierson
J. W. Poduska
C. W. Rook
J. H. Sununu
E. F. Wahl III
G. L. Wilson


## A. WORK COMPLETED

### 1. RANDOM THEORY OF TURBULENCE

This research has been completed by J. W. Poduska and the results have been presented to the Department of Electrical Engineering, M.I.T., as a thesis in partial fulfillment of the requirements for the degree of Doctor of Science, September 1962.

W. D. Jackson

### 2. HYDROMAGNETIC WAVEGUIDES

The present phase of this work has been completed and the results have been presented as theses to the departments indicated.

N. Gothard, "Excitation of Hydromagnetic Waves in Highly Conducting Liquids," S.M. Thesis, Department of Electrical Engineering, M.I.T., September 1962.

M. H. Reid, "Alfvén Waves in Liquid NaK Alloy," S.B. Thesis, Department of Electrical Engineering, M.I.T., June 1962.

R. E. Rink, "Torsional Modes in Hydromagnetic Waveguides; Some Practical Considerations," S.B. Thesis, Department of Electrical Engineering, M.I.T., June 1962.

H. M. Waller, "Design and Construction of A Hydromagnetic Waveguide," S.B. Thesis, Department of Mechanical Engineering, M.I.T., June 1962.

W. D. Jackson, G. B. Kliman

### 3. DESIGN AND CONSTRUCTION OF A MAGNETOHYDRODYNAMIC CHANNEL FLOW SYSTEM

A magnetohydrodynamic channel flow system operating on NaK alloy has been designed and constructed. The results of this work have been presented by


*This work was supported in part by the National Science Foundation under Grant G-24073, and in part by the U.S. Air Force (Aeronautical Systems Division) under Contract AF33(616)-7624 with the Aeronautical Accessories Laboratory, Wright-Patterson Air Force Base, Ohio.

F. W. Fraim III to the Department of Mechanical Engineering, M.I.T., in partial fulfillment of the requirements for the degree of Master of Science, September 1962.

W. D. Jackson, J. M. Reynolds III

## 4. A-C PROPERTIES OF SUPERCONDUCTORS

The present phase of this work has been completed by R. A. Reitman and the results have been presented in a thesis entitled "Superconducting Solenoids" to the Department of Electrical Engineering, M.I.T., in partial fulfillment of the requirements for the degree of Bachelor of Science, June 1962.

W. D. Jackson

## B. HALF-CYCLE PLASMA PARAMETRIC GENERATOR

The object of this report is to describe quantitatively the characteristics of a parametric generator in which the inductance of a resonant circuit is varied periodically by a slug of ionized gas. In previous reports,[1,2] results were presented which indicate that when the conductor does not deform the parameters needed for a mathematical analysis can be obtained from measurements or calculations based on a static system with steady-state ac excitation. These results were verified on a system with copper conductors to obtain the parameter variations.[2] This technique was used to calculate the theoretical performance of generators by using ionized gases to obtain parameter variations, and by assuming the small-signal limit of no compressibility effects.[3]

In this report we present some initial experimental results on a parametric generator using a plasma as the working fluid. An experiment has been devised with a magnetically driven shock tube used as the source of conducting gas. Only one slug of conducting gas is produced; consequently, a system was devised to use that slug of gas to examine one half-cycle of generator operation.

Because of the nature of the experiments performed, the steady-state analysis[3] is not directly usable for interpreting the results. The new mathematical model that was chosen for this purpose still retains the essential feature of the previous model[3]; namely, that parameters are determined from a mechanically static, steady-state ac analysis.

The essential results are that, as predicted by the steady-state analysis,[3] net power was generated in one half-cycle of generator operation. Although there was considerable scatter in the data points, the experimental results were predicted to a fair degree of accuracy by the new mathematical model.

### 1. Experiment

The configuration of the coil-plasma system is illustrated in Fig. IX-1. When the plasma slug enters the coil, it does work on the magnetic field, and when it leaves, work

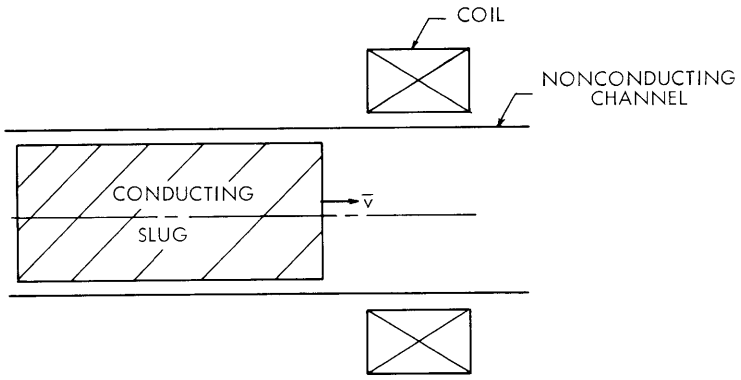


Fig. IX-1. System geometry.

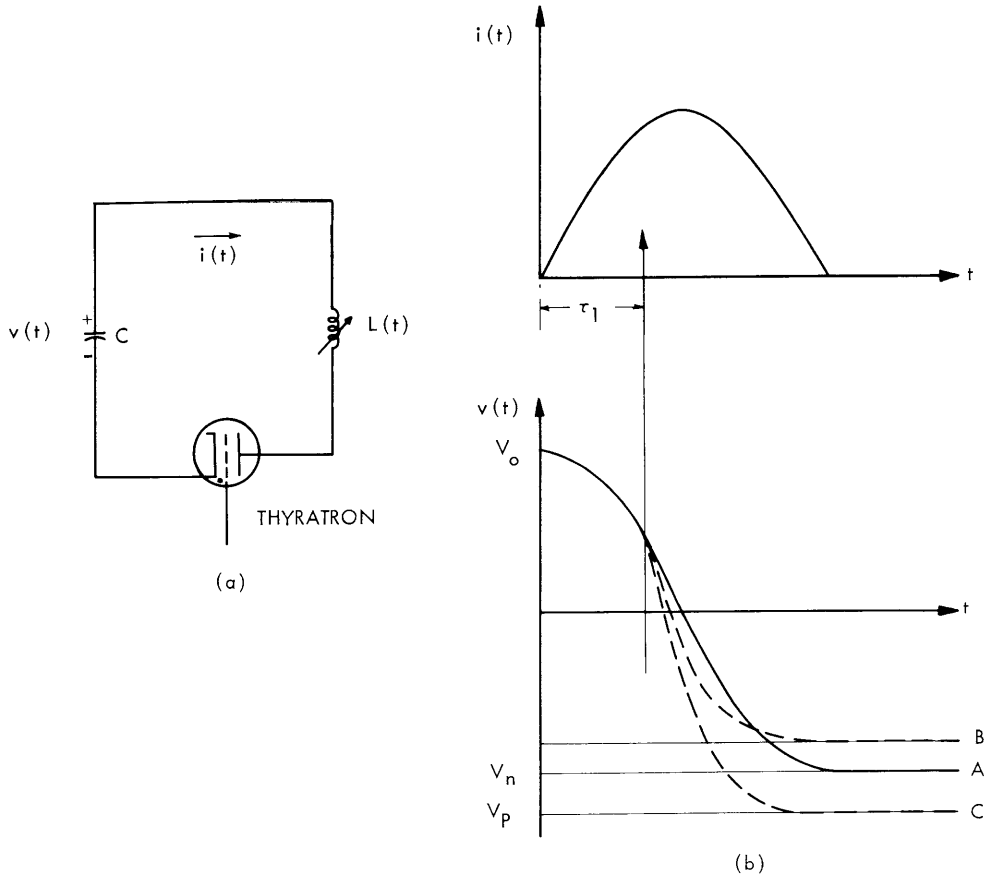


Fig. IX-2. Schematic diagram of experiment.

is done on it by the field. If the field is greater when the slug enters than when it leaves, net work has been done on the field by the slug, and energy has been converted from mechanical to electrical form. If the electrical losses in the coil and in the gas are small enough, net usable output energy may be obtained.

The experiment was performed with the circuit of Fig. IX-2a, in which L(t) is the inductance of the coil coupled to the moving plasma, capacitor C is charged to an initial voltage $V_o$, and the thyratron is used as a switch to initiate and terminate the experiment. When the thyratron is fired by a grid signal at t = 0, the voltage and current waveforms will appear qualitatively as in Fig. IX-2b. The current through the coil is roughly sinusoidal and the circuit is opened by the thyratron when the current reaches zero. The capacitor voltage is roughly cosinusoidal, as illustrated in Fig. IX-2b. The final voltage on the capacitor at the end of the half-cycle gives a direct indication of the energy conversion. For instance, curve A in Fig. IX-2b represents the system with no plasma flow. Because the coil and thyratron have losses, $|V_n| < V_o$. When the plasma traverses the coil this curve will be changed, curve B representing the result when the plasma absorbs net energy from the circuit, and curve C representing the result when net energy is extracted from the plasma. Whether curve B or C results depends on the plasma parameters (mainly the magnetic Reynolds number) and on the time, relative to the current pulse shown in Fig. IX-2b, at which the plasma enters the coil. Curves B and C indicate that the cycles end at earlier times than for curve A because the effective circuit inductance is reduced by the coupling of the coil to the plasma.

a. Experimental Procedure

The shock tube used to produce the plasma slug is an electrically driven tube, 4 inches in diameter, similar to one described in an earlier report.[4] The experiments are performed in hydrogen at an initial pressure of 0.2 or 0.3 mm Hg. The shock tube is driven by a 40-mfd bank of capacitors charged to 24 kv and discharged by an air-gap spark switch. The ringing frequency of the driving system is 125 kc. The axial length of plasma produced by the shock tube at the position of the experiment is 10-15 cm. The leading edge of the plasma at the shock front is well defined, but the trailing edge is indefinite. The lengths cited are effective lengths obtained experimentally with steady magnetic fields.

The parametric generator circuit (see Fig. IX-2a) consists of a short coil that is axially symmetric with the shock tube, a mica capacitor to give a ringing frequency of 200 kc, and a hydrogen thyratron (3C45) as a switch. The Q of the resonant circuit with the thyratron short-circuited is 30. With an initial capacitor voltage ($V_o$) of 1600 volts, a peak current of approximately 8 amps flows and yields a peak field strength of approximately 20 gauss.

To study experimentally the energy-conversion properties of the configuration of Fig. IX-2a, we found it convenient to measure the voltage on the capacitor during the transient. The ratio of final-to-initial voltage gives a direct measure of the net energy conversion. To ascertain the plasma velocity and the time at which the plasma enters the coil, a phototube was placed at each end of the coil to measure the time of arrival of the luminous gas behind the shock front. The conditions of the experiment were most easily varied by maintaining the shock velocity (and plasma properties) constant and varying the time relative to the coil-current pulse at which the plasma entered the coil.

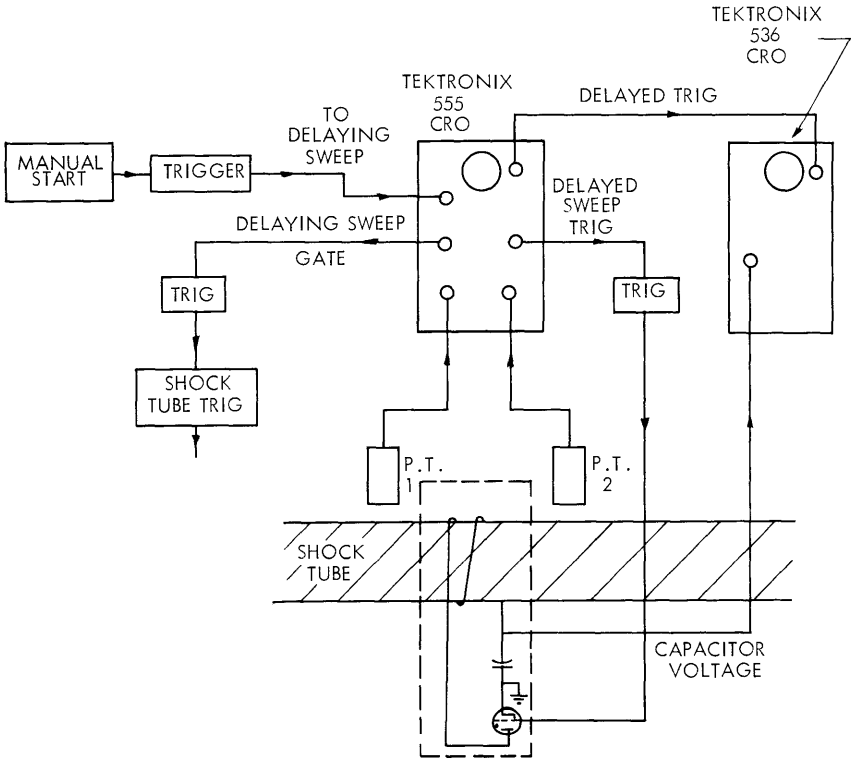


Fig. IX-3. Block diagram of experiment.

The system used to perform this experiment is illustrated in Fig. IX-3. A manually operated switch triggers the delaying sweep of the Tektronix 555 oscilloscope, and the delaying sweep gate triggers the shock tube. The variable delay in the oscilloscope is used to delay the start of the coil current until the desired time. The type 555 oscilloscope is used to record the phototube outputs and the Tektronix 536 oscilloscope is used to record the capacitor voltage. Typical oscilloscope traces are shown for the phototubes in Fig. IX-4a and for the capacitor in Fig. IX-4b. For reference, the capacitor voltage transient with no plasma is shown in Fig. IX-4b. All of the traces are started

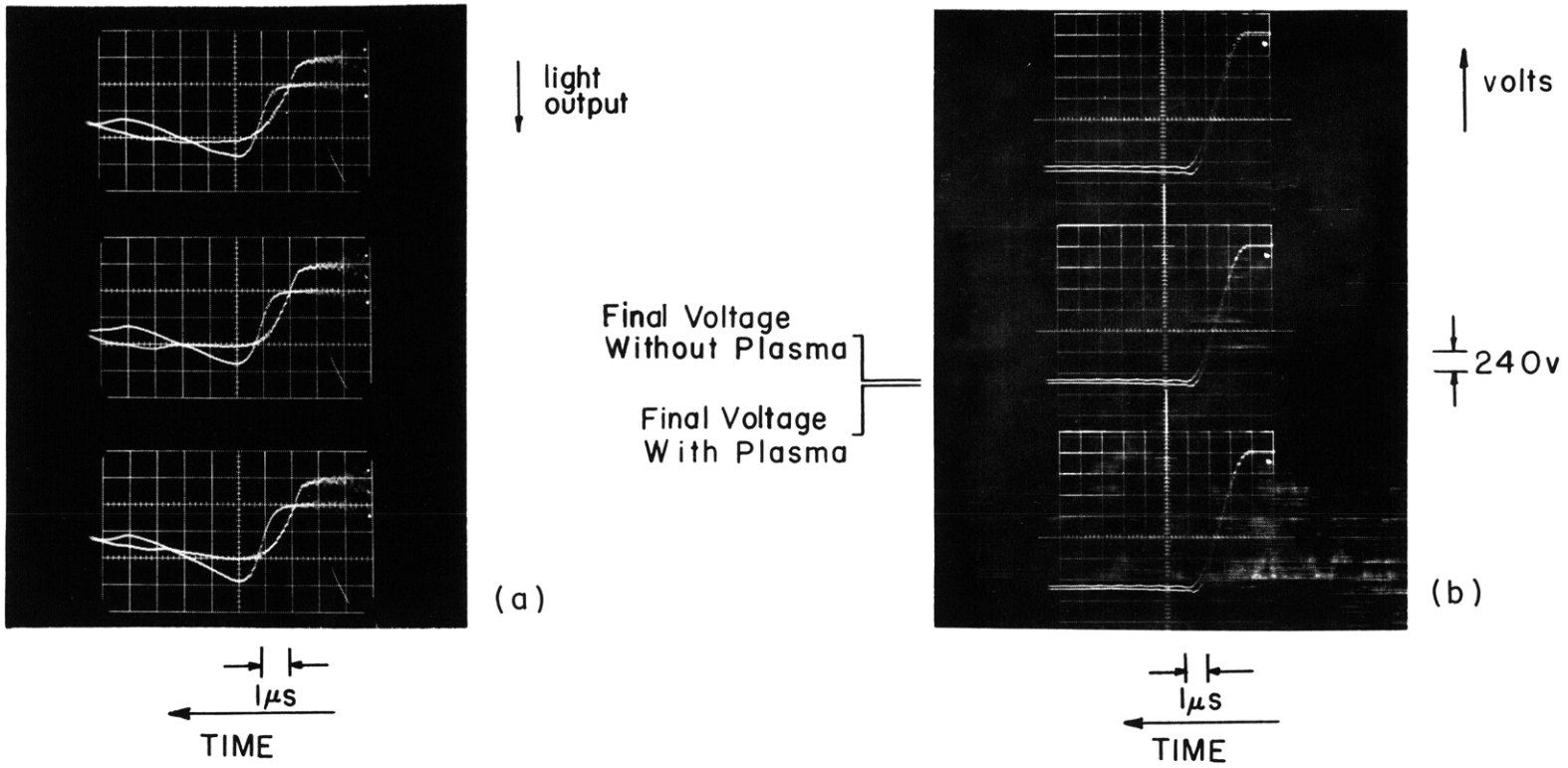


Fig. IX-4. (a) Phototube signals.
(b) Capacitor voltage.

by the delayed sweep gate of the 555 oscilloscope. There is a 0.8-μsec delay between the start of the sweeps and the firing of the generator thyratron.

The actual experimental apparatus is shown in the photographs of Figs. IX-5, IX-6, and IX-7. Figure IX-5 shows the shock tube with the generator coil, phototubes and the shielding box (with cover removed) containing the generator capacitor and thyratron. Figure IX-6 shows the oscilloscopes and other electronic circuitry in a Faraday cage that is approximately 30 feet from the shock tube. The high-voltage power supply and controls for the shock tube are shown in Fig. IX-7.

Data in the form of oscilloscope traces like those of Fig. IX-4 were taken for a variety of delays between shock-tube and generator-circuit firing times for four different shock velocities. The data were processed as follows: For each of the two phototube traces a line is drawn through the steepest slope, and the intersection with the zero level (no light) is found. This time is taken to be the time at which the shock front passes the phototube. The time of passage of the shock front between the phototubes divided into the distance between the phototubes gives the plasma velocity. The time from the beginning of the sweep (start of the generator current pulse) to the time halfway between the phototube signals is taken to be the time at which the plasma reaches the center of the coil relative to the generator current pulse. For the capacitor voltage signal the difference between the final values of the two voltages $\Delta V$ is measured and divided by the initial voltage $V_o$. This ratio is then used to find the change in $|V_p|/V_o$ above or below the final value without plasma ($|V_n|/V_o$). The value of $|V_n|/V_o$ depends only on the circuit Q and the thyratron voltage drop.

The results of four experimental runs are shown by the data points in Fig. IX-8. The shock-tube conditions were the same for all runs (hydrogen at 0.3 mm Hg and 24 kv on driver capacitors) and the variation in velocity was achieved by moving the generator coil to different positions on the shock tube. There is considerable scatter in the points, but it is evident that for some conditions $|V_p|/V_o > 1$, an indication that net energy has been converted. That is, the energy stored in the capacitor is greater at the end of the half-cycle than it was at the beginning. This increase in energy and the circuit losses were extracted from the flowing gas.

## 2. Simple Theory

The interpretation of the experimental results presented in Fig. IX-8 depends on a variation of the steady-state generator theory reported elsewhere.[3]

The assumption is made that the experiment can be represented by the circuit of Fig. IX-9. The parameters $R_1$ and $L_1$ describe the coil in the absence of the plasma. The parameters $R_{eq}$ and $L_{eq}$ describe the parameter changes that occur when the plasma completely fills the coil. All of these parameters are calculated by assuming a mechanically static system with steady-state ac excitation.[3]

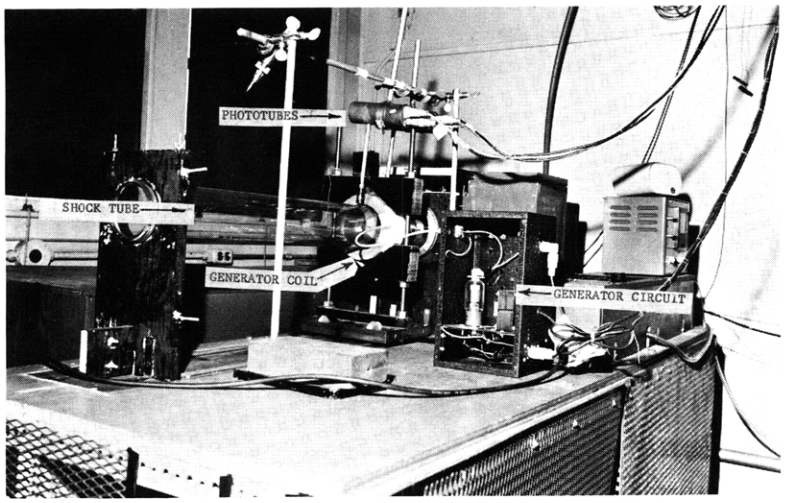


Fig. IX-5. Shock tube and generator circuit.

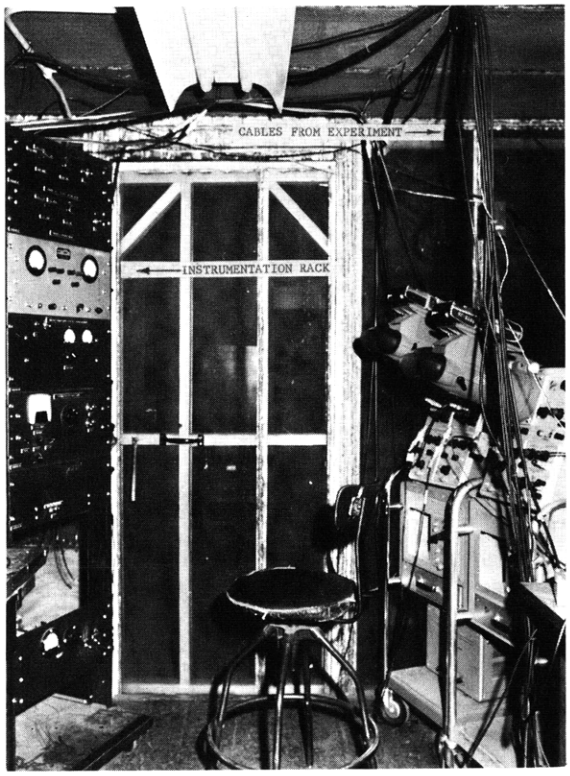


Fig. IX-6. Oscilloscopes and controls viewed from inside the Faraday cage.

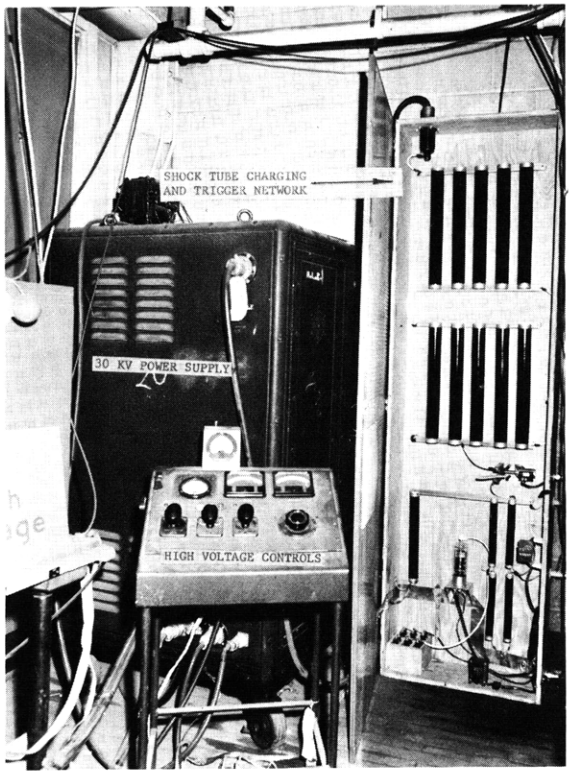


Fig. IX-7. Power supply (30 kv), instrumentation, and controls.

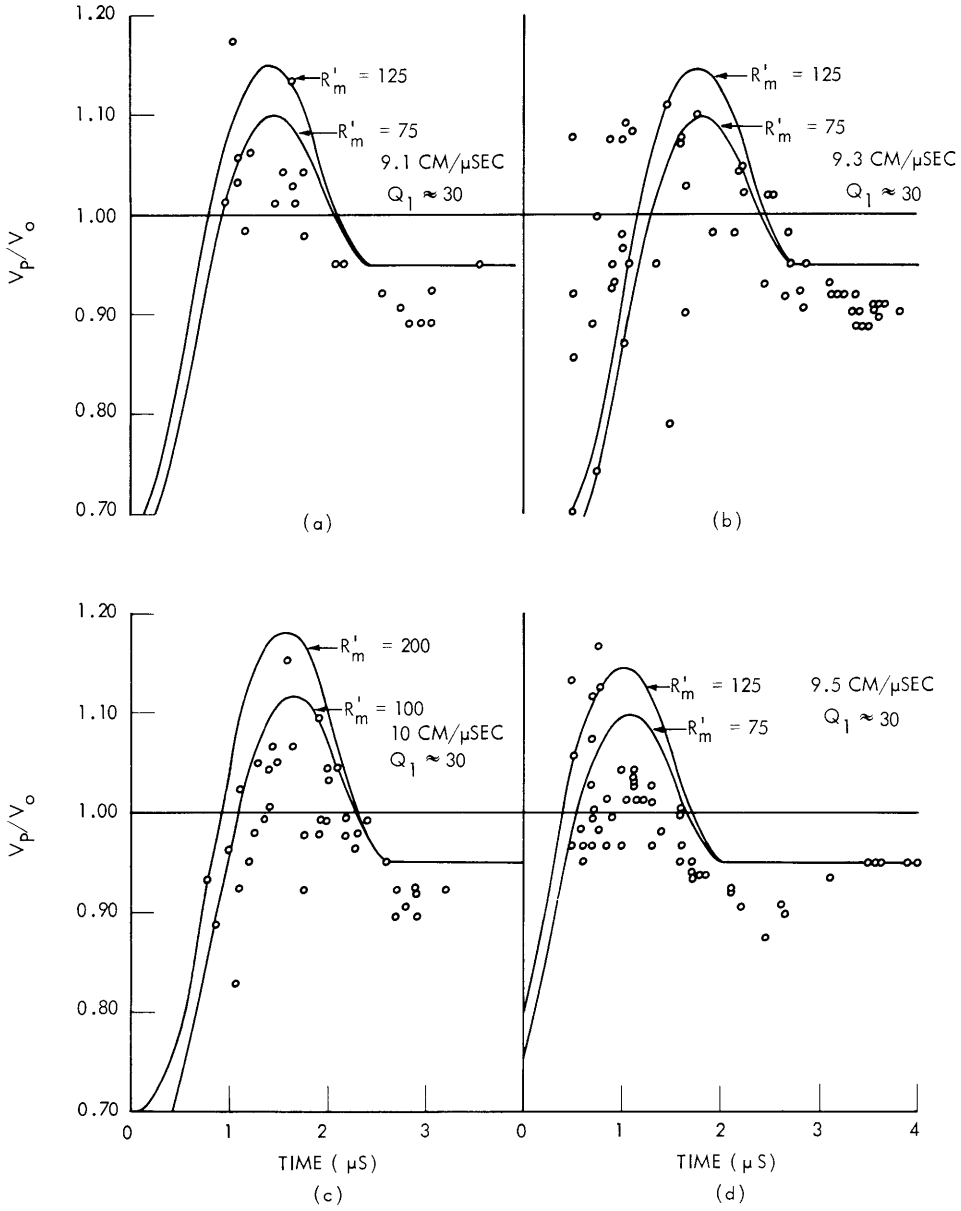


Fig. IX-8. Experimental results.

In the circuit of Fig. IX-9, switch $S_1$ represents the thyratron and is closed at t = 0 to initiate the experiment with $S_2$ closed. Switch $S_2$ is opened at $t = \tau_1$, the time at which the leading edge of the plasma reaches the center of the coil. The experiment is terminated at $t = \tau_o$, when the current goes to zero and switch $S_1$ (the thyratron) opens. It is evident that as the plasma enters the coil the effective inductance changes continuously. This continuous change is approximated here by a step change, the time of the step being at the mean time between the beginning and end of the transition. This

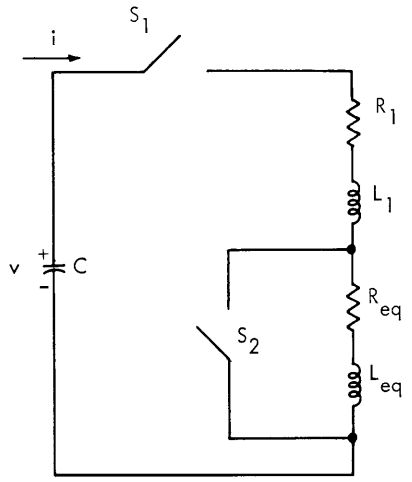


Fig. IX-9. Equivalent circuit for analysis.

approximation simplifies the analysis considerably while retaining the essential features of the conversion mechanism.

The performance of the circuit of Fig. IX-9 is calculated as follows. With switch $S_2$ closed and $S_1$ open the capacitor C is charged to an initial voltage $V_o$. Switch $S_1$ is closed at $t = 0$ and the ensuing transient is calculated. At $t = \tau_1$, switch $S_2$ is opened, thus holding flux linkages (Li) constant, and the next part of the transient is calculated. The voltage $V_p$ is a capacitor voltage at $t = \tau_o$. The analysis of this transient is a straightforward, piecewise-linear analysis and will not be repeated here. The essential results are that the final capacitor voltage $V_p$ depends only on the parameters of the coil without plasma which are given by

$$Q_1 = \frac{\omega_1 L_1}{R_1} \tag{1}$$

$$\omega_1 = \frac{1}{\sqrt{L_1 C}} \sqrt{1 - \frac{1}{4Q_1^2}} \tag{2}$$

and on the magnetic Reynolds number defined by

$$R'_m = \mu_o \sigma \omega_1 a^2, \tag{3}$$

where $\sigma$ is plasma conductivity and a is plasma radius.

Theoretical curves resulting from this theory are shown in Fig. IX-8. Two curves are shown on each graph because there is some uncertainty about the exact value of the conductivity of the plasma. The two curves represent the amount of uncertainty in $R'_m$. Although the relative entrance times $\tau_1$ in each series of data are accurate, the absolute value contains approximately 0.5 μsec of uncertainty. Consequently, the theoretical curves have been shifted in time to give the best fit.

3. Results

It is evident from the plots of theoretical and experimental results in Fig. IX-8 that the theory predicts approximately the shapes of the experimental curves but there is considerable scatter in the experimental points.

The scatter in experimental points is primarily due to plasma conditions in the shock tube. The leading edge of the plasma at the shock front is well defined but the trailing edge is diffuse and varies from shot to shot. Careful examination of the data points in Fig. IX-8 shows that for early entrance times ($0 < \tau_1 < 2$ μsec) the scatter is much more than for late entrance times ($2 < \tau_1 < 4$ μsec). The earlier the entrance time, the more the axial length of plasma is effective in the experiment. Thus, variation in axial length of the plasma from shot to shot is probably responsible for the scatter.

The absolute shock velocity can be measured with an accuracy of ± 10 per cent from the phototube traces, and the relative velocity from one shot to the next can be measured within ± 5 per cent. These errors, coupled with the strong dependence of conductivity on velocity, make the uncertainty in magnetic Reynolds number as high as ± 50 per cent in some cases.

The change $\Delta V$ can be measured from the oscilloscope trace to give an accuracy of ± 0.01 in the ratio $|V_p|/V_o$.

All of these errors lead to uncertainty and scatter in the data points. There are other sources of error that affect the agreement between theory and experiment. First, the assumption of a step change in inductance for the theory, whereas the experimental inductance changes continuously, makes the theory optimistic for early entrance times and for the peak $|V_p|/V_o$. It has already been stated that the axial length of the plasma is short enough so that for early entrance times the plasma essentially leaves the coil before the current stops flowing. This effect reduces the ratio $|V_p|/V_o$ for early entrance times and makes the theoretical curves for Fig. IX-8 optimistic.

It has been noted from experiments with steady fields that the main shock wave is preceded by a very fast, low-conductivity pulse that produces no luminosity. Such a pulse will have the effect of loading the generator coil because it traverses the coil at the wrong time and with the wrong velocity to allow energy extraction by the coil. The loading effect will be greatest for late entrance times of the main shock because there is more time during the generator current pulse for the loading to occur. This effect tends to make the theoretical curves optimistic for late entrance times.

The experimental difficulties and theoretical uncertainties cited above represent the major sources of error and scatter in the results. The key point is that each complication, neglected in the theory, would tend to decrease the ratio $|V_p|/V_o$ if it were included. Consequently, the error between theory and experiment is in the correct direction.

The major point to be made is that with an ionized gas as the working fluid, a parametric generator has produced net electrical power during one half-cycle of operation. Moreover, although the experimental conditions achieved here and the relative geometry assumed in the analysis of steady-state generator operation[3] are not identical, the results obtained here check qualitatively with the predictions made earlier.[3]

G. L. Wilson, A. T. Lewis, H. H. Woodson

References

1. H. H. Woodson, G. L. Wilson, and M. Smith, Parametric generator, Quarterly Progress Report No. 63, Research Laboratory of Electronics, M.I.T., October 15, 1961, pp. 49-55.

2. H. H. Woodson, G. L. Wilson, and A. T. Lewis, Parametric generator, Quarterly Progress Report No. 64, Research Laboratory of Electronics, M.I.T., January 15, 1962, pp. 138-142.

3. H. H. Woodson, G. L. Wilson, and A. T. Lewis, A study of magnetohydrodynamic parametric generators, Third Symposium on the Engineering Aspects of Magnetohydrodynamics, Rochester, N.Y., March 1962 (to be published).

4. H. H. Woodson and A. T. Lewis, Plasma megnetohydrodynamic experiments, Quarterly Progress Report No. 59, Research Laboratory of Electronics, M.I.T., October 15, 1960, pp. 40-45.

## C. CONTINUITY OF THE TANGENTIAL ELECTRIC FIELD IN MAGNETOHYDRODYNAMIC MACHINES

In the analysis of some models for a magnetohydrodynamic machine it is possible to obtain a discontinuity in the tangential electric field across a boundary in apparent violation of Maxwell's equations. This is due to the use of a model in which current would normally flow across a boundary but is constrained not to by conditions specified in the problem statement, for example, between two materials of different electrical conductivity in direct contact. This specification is not correct unless there is an insulating strip to prevent the flow of current. As the thickness of the insulating strip approaches zero it is found to support a dipole charge layer (double layer) across which, as shown by Stratton,[1] there is a discontinuity in the tangential electric field which is proportional to $\vec{\nabla}\tau$, where $\tau$ is the dipole surface density. The normal electric field is continuous across a dipole layer.

Another view of the source of the discontinuity is provided by the mathematical approach used in magnetohydrodynamics. The fields are determined without the use of the equation for $\vec{\nabla}\cdot\vec{E}$, which can then be used to determine the charge density. Thus the difficulty is not that the fields are incorrect, but that the proper charge density to satisfy all conditions (in this case a dipole charge layer) has not been added to the solution.

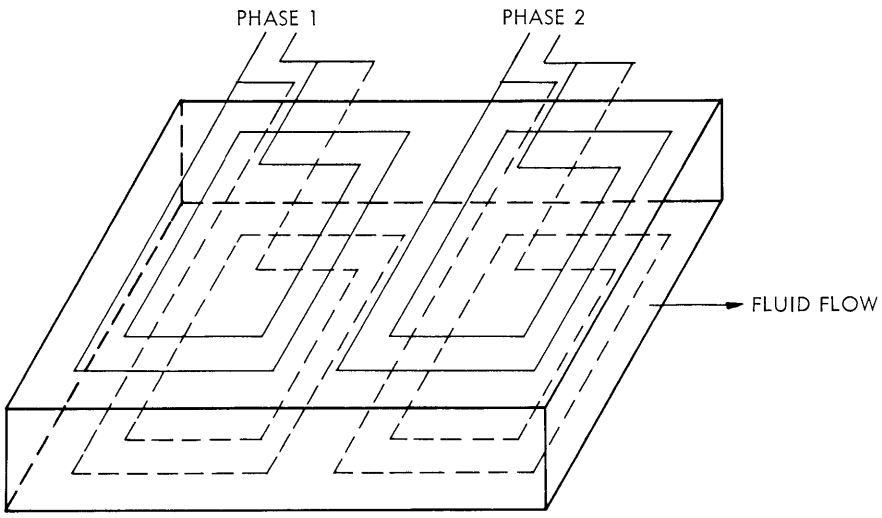


Fig. IX-10. MHD induction machine.

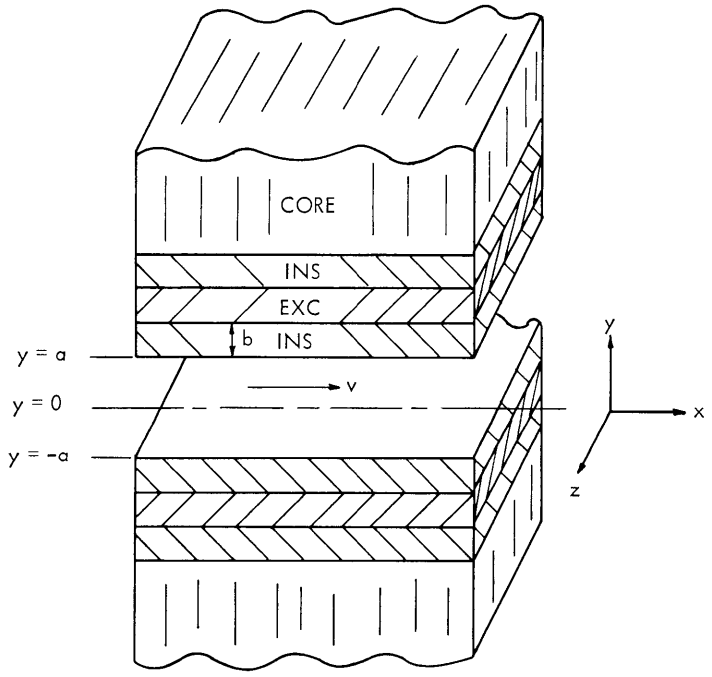


Fig. IX-11. The model.

As an illustration, consider the magnetohydrodynamic induction machine shown schematically in Fig. IX-10. The model to be analyzed, shown in Fig. IX-11, is infinite in the x and z directions. The fluid velocity is assumed to be constant, and in the x direction (slug flow) to uncouple the electromagnetic and fluid equations and thus allow an analytical solution to be obtained. The exciting plates, separated from the fluid and

core by insulating strips, are driven by a current source that gives a symmetric current density,

$$\vec{J}_e = \vec{i}_z J_o \cos(\omega t - kx), \tag{1}$$

which represents a traveling current wave of amplitude $J_o$, frequency $\omega$, and wavelength $\lambda = 2\pi/k$. The current is considered to be produced by a balanced n-phase system with n greater than one. The exciting plates are made of fine insulated wire so that current can flow only in the z direction.

The electromagnetic fields are determined from Maxwell's equations with the usual magnetohydrodynamic approximation of neglecting displacement currents. The analysis is simplified by the use of a vector potential $\vec{A}$ and a scalar potential $\phi$ defined by

$$\vec{B} = \vec{\nabla} \times \vec{A} \tag{2}$$

$$\vec{E} = -\vec{\nabla}\phi - \frac{\partial \vec{A}}{\partial t}. \tag{3}$$

Noting that Ohm's law in a moving fluid is $\vec{J} = \sigma(\vec{E}+\vec{v}\times\vec{B})$ and substituting Eqs. 2 and 3 in Maxwell's equations gives

$$\nabla^2\vec{A} - \mu\sigma\frac{\partial \vec{A}}{\partial t} + \mu\sigma(\vec{v}\times\vec{\nabla}\times\vec{A}) = 0 \tag{4}$$

$$\nabla^2\phi - \mu\sigma\frac{\partial \phi}{\partial t} = 0. \tag{5}$$

Here,

$$\vec{\nabla}\cdot\vec{A} + \mu\sigma\phi = 0 \tag{6}$$

has been chosen to uncouple Eqs. 4 and 5. The x- and t-dependence of all quantities must be as $e^{j(\omega t-kx)}$ from the excitation and boundary conditions. This will not be indicated explicitly. $\vec{A}$ is due solely to currents, so that it, as well as $\vec{J}$, is in the z direction and independent of z. The inclusion of all components of $\vec{A}$ will not affect the fields obtained.

For symmetric excitation the electric field in the fluid is

$$\vec{E}_f = -\vec{i}_z jA_1 \cosh \gamma y. \tag{7}$$

$A_1$ is determined from the boundary conditions on the magnetic field and is a function of the machine parameters and dimensions, but not of the conductivity of the exciting sheets. In the exciting sheets $E_{ez} = J_o/\sigma_e$. It is obvious that without the insulating strip $E_{fz}$ and $E_{ez}$ will not match at the boundary. This is the case considered by Bernstein et al.,[2] who found such a discontinuity.

With the addition of the insulators the complete problem has to be solved. This

addition adds a scalar potential that exists only in the insulators and allows all conditions to be satisfied. For small b, (bk « 1), the change in the tangential electric field across the insulating strips, $\Delta E_z$, may be written as

$$\Delta E_z = E_z(c) - E_z(a) = -j\omega A_1 \gamma b \sinh \gamma a + \frac{\phi_1 kb}{\sinh ka} . \tag{8}$$

where $\phi_1$, a constant determined from machine parameters, is due to the scalar potential in the insulator. For small b, $A_1$ remains finite but $\phi_1$ varies inversely as b. In the limit, $\Delta E_z$ becomes

$$\lim_{b\to 0} \Delta E_z = \frac{J_o}{\sigma_e} + j\omega A_1 \cosh \gamma a , \tag{9}$$

which is the discontinuity encountered without the insulator. The product of b and the surface charge density on the insulator becomes independent of b for small b; the insulator supports a dipole charge layer that results in the discontinuity of $E_z$. Note that $E_x$ is also discontinuous and that a similar discontinuity exists between the core and exciting plates.

The results of Bernstein et al.[2] are thus correct. They have implicitly assumed an insulating strip of infinitesimal thickness in their model. The present analysis is necessary to justify their work and to allow extensions to more exact models. Similar problems arise at the exciting windings in connection with magnetohydrodynamic wave machines.[3] This type of boundary condition is also of interest in electrohydrodynamics.[4]

E. S. Pierson

References

1. J. A. Stratton, Electromagnetic Theory (McGraw-Hill Book Company, Inc., New York, 1941), pp. 188-192.

2. I. B. Bernstein, J. B. Fannucci, K. H. Fishbeck, J. Jarem, N. I. Koram, R. M. Kulsrud, M. Lessen, and N. Ness, An electrodeless MHD generator, Second Symposium on the Engineering Aspects of Magnetohydrodynamics, University of Pennsylvania, Philadelphia, March 9-10, 1961, edited by C. Mannal and N. W. Mather (Columbia University Press, New York, 1962), p. 260.

3. A. J. Schneider (private communication, July 1962).

4. J. R. Melcher (private communication, July 1962).

## D. WORK FUNCTION OF MONOCRYSTALLINE TANTALUM IN A CESIUM VAPOR

The work function of the (110) face of a single crystal of tantalum exposed to a vapor of cesium was estimated experimentally. The saturation temperature of the vapor was between 320°K and 380°K; the range of temperatures of the crystal surface was 1100°K to 1300°K. My method was to construct a planar diode, made with single-crystal electrodes, and to measure the saturated thermionic electron emission. From this

measurement I calculated the effective work function by substitution in Richardson's equation.

The envelope of the tube was glass, and the emitter was heated by electron bombardment. A screen eliminated edge effects. The results indicate that the work function of the cesium-covered surface is $\sim 0.3$ ev lower than that of the polycrystalline material under the same conditions of cesium vapor and surface temperature. This result corresponds to theoretical predictions based on the work function of the bare metal which was found to be $4.75 \pm .05$ ev.

This work is described in extenso in the author's thesis.[1]

W. T. Norris

References

1. W. T. Norris, Thermionic Emission from a Single Crystal of Tantalum Exposed to Cesium Vapor, Sc.D. Thesis, Department of Mechanical Engineering, M.I.T., September 1962.

## E. ELECTRICAL CONDUCTIVITY OF A NONEQUILIBRIUM PLASMA*

A theory of electrical conduction in nonequilibrium plasmas has been presented elsewhere.[1] It differs from previous theories in recognizing that the increased ionization that results from the elevation of electron temperature by ohmic heating may, under certain conditions, be closely coupled to the electron temperature through a Saha type of equilibrium, if the electrons have a Maxwellian energy distribution, and the dominant ionization process is electron-atom collisions.

One type of plasma that is of interest for magnetohydrodynamic generators and accelerators is a mixture of noble gas and alkali metal at pressures that are slightly below 1 atmosphere and temperatures between 1500°K and 3000°K. Such a plasma satisfies the requirements stated above. Furthermore, it has been shown[2] that a large increase in electron temperature can be attained in a magnetohydrodynamic generator by utilizing such a plasma as working fluid.

Kerrebrock's theory[1] was qualitatively checked by an experiment in which the plasma was produced by an arc and seeded by adding gas that had been bubbled through molten potassium. Both the arc and the seeding method introduced considerable uncertainty in the determination of the composition of the plasma.

The goal of the present work is to measure precisely the conductivity of noble gas-alkali metal plasmas under the conditions described above. Thus far, preliminary

*This research was supported in part by the U.S. Air Force (Office of Scientific Research of the Office of Aerospace Research) under Research Grant No. 62-308.

measurements have been carried out in a very pure, 2000°K argon-potassium plasma produced in a tantalum heat exchanger. The conductivity was measured with tantalum electrodes for various potassium concentrations.

The counterflow heat exchanger is shown schematically in Fig. IX-12. It is heated by nitrogen from an arc. Its outer structure is of graphite, insulated with carbon batting. The tantalum inner tube ends inside a glass jar that contains the electrode assembly. In a lead bath at approximately 800° C the argon is preheated and seeded with potassium vapor, which is metered through a choked orifice from a small boiler. The plasma temperature is measured with a pyrometer focused on the exterior of the hot end of the tantalum tube that is enclosed by a graphite structure in order to approximate a black body. (The cavity and thermocouple shown in Fig. IX-12 will be used in future experiments.)

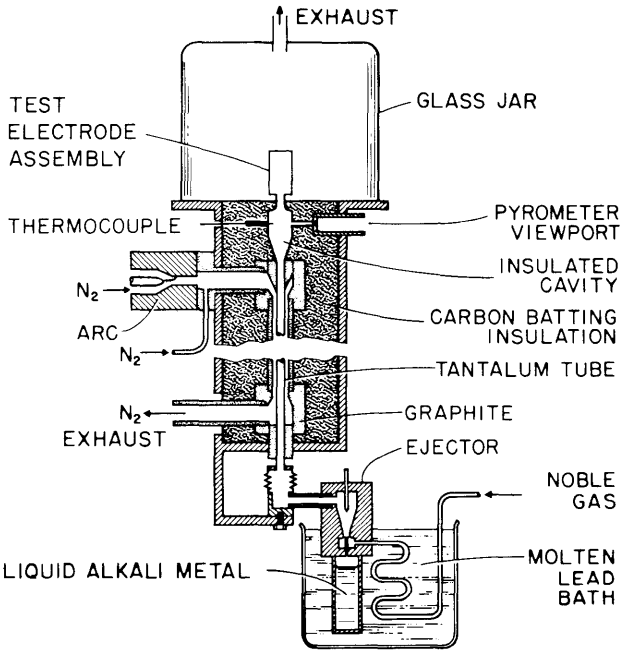


Fig. IX-12. Schematic diagram of heat exchanger, potassium seeder, and test electrode assembly.

The test electrode assembly is shown in Fig. IX-13. Two ring-shaped electrodes are supported by a boron nitride tube that is heated by a tungsten heating element. This assembly is mounted at the top of the heat exchanger.

The measured electrical conductivity of the plasma is shown in Fig. IX-14. The principal parameter in the curves is the potassium concentration. The points on each curve were obtained by increasing the current in stepwise fashion and then decreasing

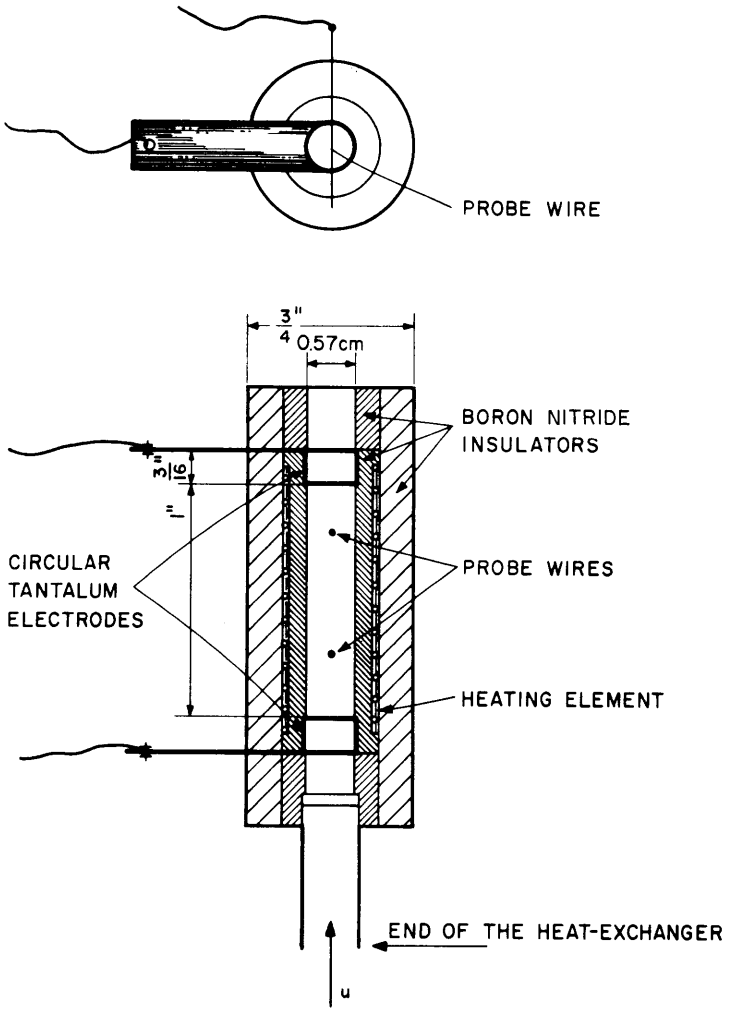


Fig. IX-13. The circular tantalum electrodes, the direction of the plasma velocity u, and the probe wires that will be used to measure the electric field gradient.

it. There is a definite hysteresis, which is thought to be due to transient heating of the electrodes. We trust that this effect will be eliminated in later experiments.

Kerrebrock's theory[1] indicates that the conductivity should be representable as a function of gas temperature and current density by a relation of the form $\log \sigma = b(T) + \alpha \log j$, where b and $\alpha$ are nearly constant over a wide range of T and j, and $\alpha$ depends only on the electron temperature. Figure IX-14 shows that $\alpha$ is nearly constant. The experimental value of $\alpha$ is also very close to that predicted by the theory.

The absolute magnitude of the measured $\sigma$ is compared with the theoretical prediction (both for constant electron temperature) in Fig. IX-15. In the theoretical

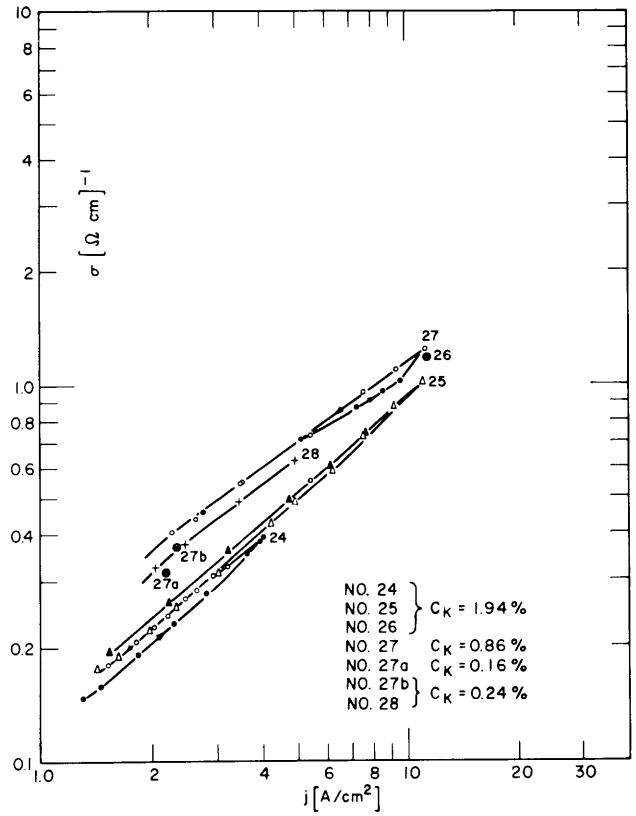


Fig. IX-14. Measured electrical conductivity of plasma vs current density. $C_K$, relative concentration of potassium in the argon stream.

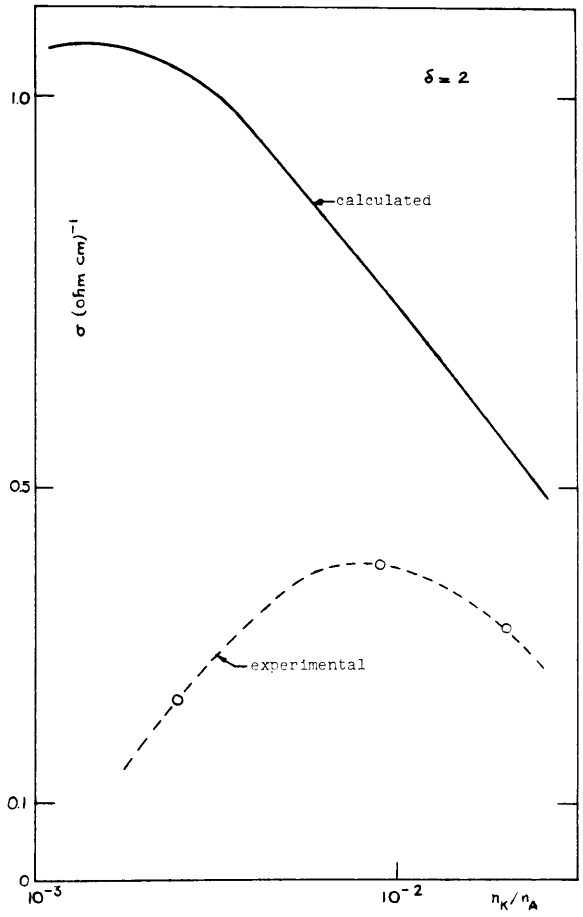


Fig. IX-15. Comparison of the measured conductivity with theory at constant electron temperature.

prediction, cross sections for argon and potassium of $0.6 \times 10^{-16}$ cm$^2$ and $0.4 \times 10^{-13}$ cm$^2$ were used. The mean electron-energy loss per collision was assumed to be $\delta(M_e/M_a)(3/2)(kT_e - kT_a)$, where $M_e$ and $M_a$ are the electron and atom masses, $T_e$ and $T_a$ are the electron and atom temperatures, and $\delta$ is assumed to be 2. Only for the point of highest potassium concentration was the potassium concentration known with good accuracy. For this point the measured conductivity is within approximately 60 per cent of the (completely theoretical) prediction with the effect of elevated electron temperature included.

This work will continue. It has been described in greater detail by Dethlefsen and Drouet.[3]

J. L. Kerrebrock, M. A. Hoffman, G. C. Oates,
R. Dethlefsen, G. A. Drouet

## References

1. J. L. Kerrebrock, Conduction in gases with elevated electron temperature, Engineering Aspects of Magnetohydrodynamics (Columbia University Press, New York, 1962), pp. 327-346.

2. H. Hurwitz, Jr., G. W. Sutton, and S. Tamor, Electron heating in magnetohydrodynamic power generators, Am. Rocket Soc. J. 32, 1237 (1962).

3. R. Dethlefsen and M. Drouet, Measurement of Electrical Conductivity in Non-Equilibrium Argon-Potassium Plasma, S.M. Thesis, Department of Aeronautics and Astronautics, M.I.T., September 1962.